Theses of Doctoral (Ph.D.) Dissertation

STUDYING THE TOXICITY AND TESTING OF NANOSIZE ELEMENTAL SELENIUM

Khandsuren Badgar

Ph.D. candidate

Dissertation supervisor:

Dr. József Prokisch, Ph.D

UNIVERSITY OF DEBRECEN

Doctoral School of Animal Science

Debrecen, 2022

1. INTRODUCTION

Selenium is an essential biological element that lends much support to health maintenance and disease prevention of humans and animals as selenocysteine in the active site of several selenoproteins including glutathione peroxidase, thioredoxin reductase, and deiodinases. However, not all organisms can produce it, so it should be taken from food for health reasons. Selenium intake by animals and humans in various countries, including in Western Europe, and East and Central Africa, is still low, leading to selenium deficiency and adverse health effects (ROEKENS et al., 1986; MARTIN et al., 2006; RAYMAN, 2012). Notably, the nutritional value of selenium depends primarily on the dose and chemical forms of selenium present in the source. Because there is a narrow gap between essential and toxic effects of selenium in animals and humans. Numerous studies reported that selenium nanoparticles (SeNPs) are more bioavailability (WANG et al., 2007; ZHANG et al., 2008; SHI et al., 2011), and much less toxic (ZHANG et al., 2008; BENKŐ et al., 2012) than other common forms. Therefore, the synthesis of selenium nanoparticles and their applications have received increasing attention in recent years.

The present work aims to produce different selenium nanoparticles and seek their applicability in the agricultural sector. Therefore, the following specific objectives have been pursued throughout the research.

❖ To synthesize selenium nanoparticles by biological and chemical methods
❖ To study the toxic and antidote effect of selenium nanoparticles with an animal model
❖ To test selenium nanoparticles in the production of nanofibrous membrane.

2. MATERIALS AND METHODS

2.1. Production of selenium nanoparticles

2.1.1. Biological method

Selenium nanoparticles were synthesized by *Lactobacillus acidophilus* (LA-5) according to Prokisch and Zommara (2011). In the procedure, 10,000 mg/L of sodium hydrogen selenite ($NaHSeO_3$) as a stock solution and 1000 mL of sterilized MRS broth as a culture medium were prepared at the same time by the method. After cooling the medium to 25 °C, 20 mL of selenium solution was mixed with 980 mL of MRS broth, which means around 200 mg/L selenium. Then 10 mL of activated bacterial culture was added to them, and the mixture solution was placed into the shaking incubator at 37 °C for 36–48 hours in aerobic condition. The color of the culture medium becomes red at the end of the fermentation process because of the converted elemental selenium. In the purification of the synthesized selenium nanoparticles, the culture medium was centrifuged at 6,000 rpm for 10–15 minutes, and the pellets were washed with distilled water, repeatedly. The selenium nanoparticles were synthesized mainly intracellular in lactic acid bacteria. Thus, 100 mL of purified selenium nanoparticles were mixed with 150 mL of 37% hydrochloric acid to lysis bacterial cell wall. At the end of the hydrolysis, the mixture solution was centrifuged at 6,000 rpm for 10–15 minutes and washed with purified water until its pH returned neutral. Finally, the washed samples were ultrasonicated for 10–15 minutes to disintegrate the cohesive selenium spheres and filtered through a vacuum filter with one plastic filter layer and two paper layers to remove the remaining bacterial cell wall.

2.1.2. Chemical method

A modified reduction method was applied in the chemical synthesis of selenium nanoparticles. In a typical procedure, sodium selenite as selenium precursor was dissolved in distilled water by various concentrations like 25 mg/L, 50 mg/L, 100 mg/L, 150 mg/L, 200 mg/L, 250 mg/L, and 500 mg/L. Ascorbic acid as a reducing agent was dissolved in the same solvent by 1 g/L, 5 g/L, and 10 g/L concentration before 2 hours of the experiment. Each concentration of stock solutions is mixed in equal proportions in a

plastic tube at room temperature for 1 hour. The mixed reactions were reacted with each other in a concentrated form until a color change from colorless to red was observed.

2.1.3. Characterization

UV/vis spectroscopy

The absorbance of the sample is determined by UV/Vis spectrophotometry (PerkinElmer Lambda2S) using a quartz cuvette (1 cm) at the ambient temperature. Pure water was applied as a control. In this method, the turbidimetry signal was measured because the signal is derived from the light scattering of solid particles rather than light absorption. Early solutions (sodium selenite and ascorbic acid) are not absorbed in 400 nm, but the nanoparticles formed can scatter light and reduce intensity.

Dynamic light scattering

The particle size distribution of the generated selenium nanoform was measured by dynamic light scattering techniques (Malvern Mastersizer 2000 particle size analyzer). This analyzer operates in conjunction with an optical bench to detect the actual scattering pattern from the particle field. The selenium nanoparticle's samples prepared at the varying rotation speeds were reported in the ranges from 0.01 µm to 1000 µm, under the following conditions: 1.33 for water refractive index, 1.590 for particle refractive index 0.01 for particle absorption coefficient, and room temperature. Furthermore, it calculates the particle size distribution from the light scattering data.

X-ray diffraction analysis

The phase composition and structure of samples were examined by X-ray powder diffraction (XRD), operating on a SuperNova X-ray diffractometer (Rigaku Corporation, Tokyo, Japan) with Cu Kα source (λ = 0.15406 nm). Crystallographic identification was achieved by comparing the experimental pattern (XRD) with the pattern in the Joint Committee on Powder Diffraction Standards (JCPDS) database.

Scanning electron microscope and energy-dispersive X-ray spectroscopy

The morphology, distribution of selenium nanoparticles, and thickness and surface of coated PVC and silicone tubes were characterized by a scanning electron microscope (SEM) using Hitachi S-4300 field emission scanning electron microscope. Energy-dispersive X-ray spectroscopy (EDS) was used to measure the elemental composition on the surface of the samples after coating. For sample preparation, small pieces of PVC and silicone tubes coated with selenium nanoparticles were rinsed with absolute ethanol and distilled water repeatedly to remove uncoated particles and other contamination. Finally, samples were dried at room temperature.

Atomic fluorescence spectrometry

Selenium concentration was measured using Millennium Excalibur (PSA, England) atomic fluorescence spectrosmetry (AFS) according to methods published and validated by instrument manufacturers (PS ANALYTICAL, 1999). For the hydride formation reaction, two solutions were used at a flow rate of 1.5 mL/min to generate the selenium hydride. The first is 3M hydrochloric acid and the second is 1.4% (w/v) sodium borohydride dissolved in 0.1M sodium hydroxide. The formed H_2Se gas was purged with 15 liters/min of argon in a double-membrane separator unit called PermaPure. By burning the diffused gas and illuminating it with monochromatic light from a hollow cathode lamp, the selenium in the flame is excited and emits fluorescent light perpendicular to the plane of the incident light. During the measurement, a 30 second sample aspiration was followed by a 30 second background wash. Each measurement was repeated 3 times, using the Charlau selenite standard for calibration. For sample preparation, 1 mL of selenium sample was mixed with 5 mL of nitric acid (65% w/w) at 60 °C for 60 minutes. After that 3 mL of hydrogen peroxide (30% w/w) was added for further destruction for 4 hours at 120 °C. The samples were then diluted to 15 mL with 3M hydrochloric acid and filtered through filter paper.

2.2. Determination of antidote effect of selenium nanoparticle

The starter culture of *P. caudatum* was multuplied in tap water supplemented with yogurt powder (1 g/L) at room temperature for 15 days. Yogurt was produced by a starter culture (Lyofast Y 250), which includes *Streptococcus thermophilus* and *Lactobacillus*

delbrueckii ssp. bulgaricus was obtained from SACCO Srl (Italy). The biological synthesized red selenium nanoparticles, which contained 800 mg/L selenium in the form of 250 nm were used in this experiment. Silver nanoparticles (AgNPs) with a concentration of 20 mg/L and a particle size of 10 to 20 nm, silver nitrate (AgNO$_3$), sodium hydrogen selenite (NaHSeO$_3$), and sodium selenate decahydrate (Na$_2$SeO$_4$ x 10H$_2$O) were used as toxicants.

2.2.1. Determination of the toxic level

Initial solutions of 20 mg/L of silver nanoparticles and silver nitrate and 80.0 mg/L of sodium selenite and sodium selenate were made and then diluted in serial dilutions (up to 10^{-10}). The exact amount of Paramecia's culture (20 µL) with toxic solutions (20 µL) was mixed on the microscope slides while monitoring by microscope in control groups. An optical microscope attached to a CCD camera monitors their locomotion, morphology, and mortality. LC95 values for all toxicants were determined, considering the lethal concentration. For liquids, LC50 or LC95 is used instead of LD50 or LD95. Calculate the LC50 concentration value by applying the effects of survival time and concentration. The LC50 value is the concentration when the survival time is 12.5 minutes. The NOEL (No Observed Aid) concentration was defined as when survival was greater than 20 minutes.

2.2.2. Determination of antidote effect of selenium nanoparticles

P. caudatum has been supplemented with selenium nanoparticles. In a typical process, 500 µL of culture was mixed with the same amount of selenium nanoparticles and kept at room temperature for around 2 hours in experimental groups. After supplementation, 20 µL of the supplemented culture was dropped in the center of a glass slide, and 20 µL of toxicants was added to them while monitoring under a microscope. At the same time, the survival time, locomotor behavior, and morphological changes of *P. caudatum* are continuously monitored by the camera. Survival vs. concentration has a unique shape that resembles a pH titration curve. The turning point gives the LC50 value. An optical microscope attached to a CCD camera and an SEM with X-ray diffraction analysis indicated the accumulation of the selenium nanoparticles in the cell.

2.3. Production of selenium nanoparticles enriched nanofibers

Preparation of polymer solution

Various concentrations (from 6% to 15%) of polyvinyl butyral (PVB) polymer was dissolved in 96% of ethanol with constant stirring (Heidolph RZR 252) at room temperature until the solution became clear. Then, the solution was left unstirred for at least 1 day.

Enrichment of polymer solution with selenium nanoparticles

PVB polymer solution was enriched with red and grey nanopowder and in-situ synthesized selenium nanoparticles. 1%, 3%, 5%, and 10% (*w/v*) red and grey selenium nanopowder were suspended in PVB polymer and sonicated for 30 minutes to obtain a homogeneous solution (Figure 1A, B). The third polymer solution was prepared by the in-situ synthesis method. In the conversion procedure, sodium selenite as a precursor and the ascorbic acid as a reducing agent were separately dissolved in 80% ethanol with 20% water, followed by a 10% PVB polymer. After dissolving, these solutions were mixed at room temperature in equal proportions, and the mixture was retained for about one hour until red (Figure 1C).
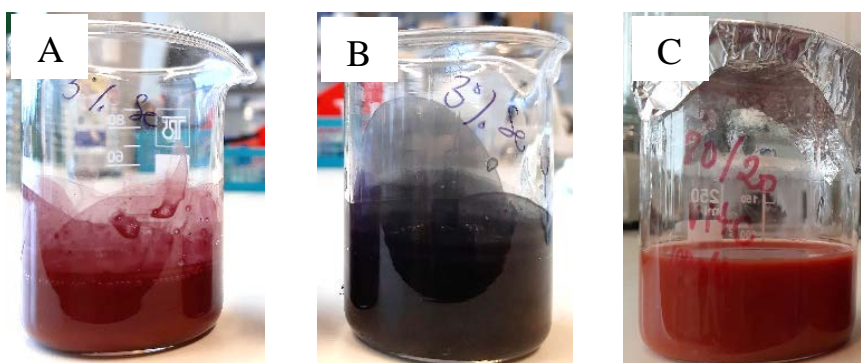

Figure 1: **PVB polymer solution suspended with red-SeNPs (A), grey-SeNPs (B), and in-situ synthesized SeNPs (C)**

Electrospinning

Selenium nanoparticles enriched nanofibers at various concentrations were produced by horizontal electrospinning setup with the following conditions. The polymer solution was placed in the syringe of 50 mL and injected at a flow rate of 10 mL h^{-1} through a

stainless-steel blunt needle. The nanofibers were collected in a stainless-steel collector located 25 cm from the tip of the needle under a voltage of 40 kV at the humidity 34% and temperature at 24 °C.

Characterization

The morphology, microstructure, surface, and chemical composition of nanofibers were analyzed by scanning electron microscopy (SEM), Energy-dispersive X-ray spectroscopy (EDS), and simple light microscope. The samples were harvested on a stainless-steel collector covered with textiles and glass slides for characterization. The fiber length is calculated according to the following equation:

$$l = \frac{4V}{d^2\pi}$$

where "l" is the fiber length in meters, "V" is the volume in m^3, "d" is the diameter in meters.

3. RESULTS

3.1. Production of selenium nanoparticles

As our results show (Figure 2), there was no reaction between 1 g/L of ascorbic acid and all concentrations of sodium selenite, and no color change was observed for more than 1 hour. In 5 g/L of ascorbic acid, moderate reduction of selenite was observed, but not sufficient. The reaction between 10 g/L of ascorbic acid and 500 mg/L of selenite was significantly better than other concentrations, indicating color changes from clear white to deep red. The red color was obtained from 6 minutes of the reaction time. The color changes of the reaction from yellow to deep red are associated with the increase in particle size (LIN and CHRIS WANG, 2005), and red color indicates amorphous selenium nanoparticles in shape (HAGEMAN et al., 2017). The color changes demonstrate the reaction rate, which was correlated with hydrogen ion concentration (pH). The reduction process is faster in acidic environments with high ascorbic acid concentrations (pH <7.0).
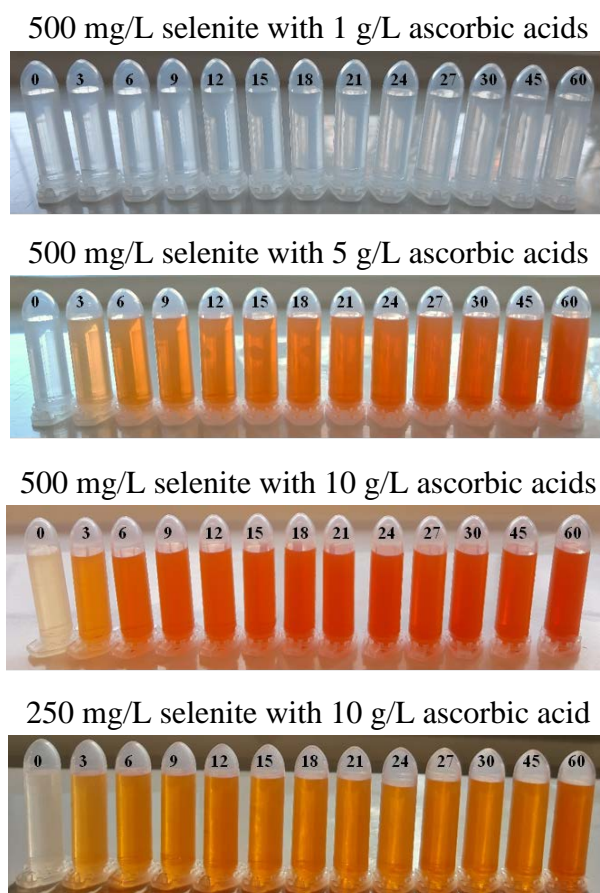
500 mg/L selenite with 1 g/L ascorbic acids

500 mg/L selenite with 5 g/L ascorbic acids

500 mg/L selenite with 10 g/L ascorbic acids

250 mg/L selenite with 10 g/L ascorbic acid

Figure 2: **Color changes of reaction between sodium selenite and ascorbic acid by reaction time**

The reduction process was measured at 400 nm by UV-visible spectrophotometry. The concentrations of ascorbic acid in 1 g/L and 5 g/L were not suitable for the reduction reaction with concentrations of selenite from 25 mg/L to 500 mg/L. Incredibly, there was no reaction between 1 g/L of ascorbic acids with all concentrations of sodium selenite. The reaction rate between 10 g/L of ascorbic acids with concentrations of sodium selenite in 25 mg/L to 500 mg/L was significantly higher than 1 g/L and 5 g/L of ascorbic acids. For concentrations of selenium precursor, the absorption of 500 mg/L of sodium selenite was dramatically increased until 30 minutes of the reaction time, as exhibited in Figure 3. These data indicated that the reaction of 500 mg/L of sodium selenite and 10 g/L of ascorbic acids are suitable for forming selenium nanoparticles.
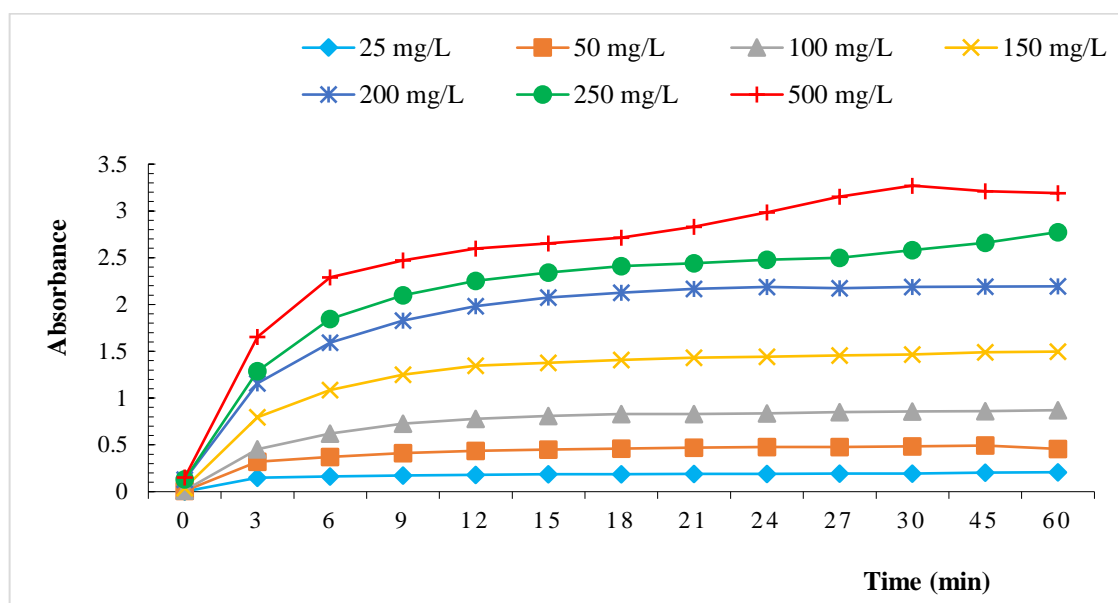

Figure 3: **Reaction rate of selenite with ascorbic acid (10 g/L) for the formation of SeNPs**

The particle size distribution of selenium nanoparticles obtained from the reaction of 500 mg/L sodium selenite and 10 g/L ascorbic acids is measured. The synthesized nanoparticles with a size range from 100 nm to 100 µm are detected. Nanoparticles can aggregate in higher concentrations in liquid form, as determined by particle size analysis. The different measurements for the aggregation were carried out after 10, 20, and 30 minutes of mixing selenite and ascorbic acid with continuous stirring (Figure 4). Over time, the size of the aggregate increased and finally reached a size of 100 µm.
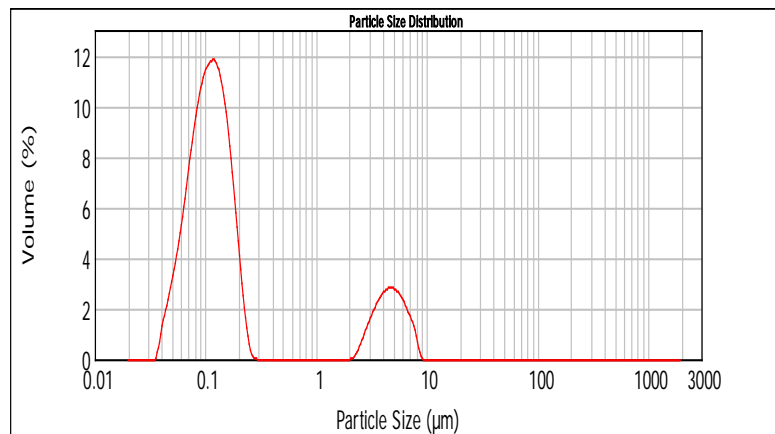
10 minutes

20 minutes
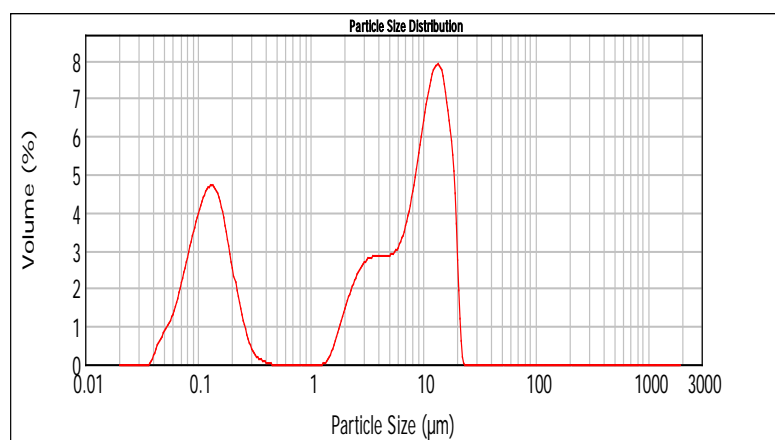
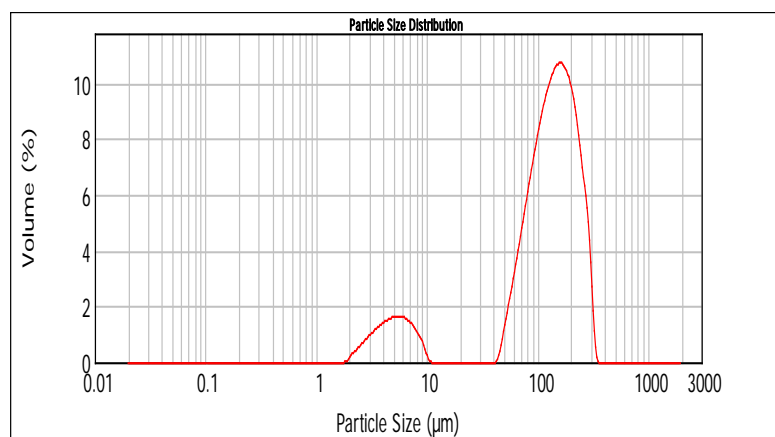30 minutes

Figure 4: **The particle size distribution of SeNPs by reaction time**

3.2. Coating of selenium nanoparticles

The selenium layer in the inner surface tube was created by a circulating flow of selenium nanosuspension solution using a peristaltic pump with a flow rate of 1–10 ml/min or 95 rpm at room temperature for 30 minutes. Also, the selenium nanolayer with

crystal structure was converted at a higher temperature of 85 °C from the red selenium-coated tubes. During the heat treatment, the red selenium-coated tube (Figure 5B) turned into the grey tube, as presented in Figure 5C. In this process, the color change is visible, and it indicates the formation of grey hexagonal selenium on the inner surface of the tube.
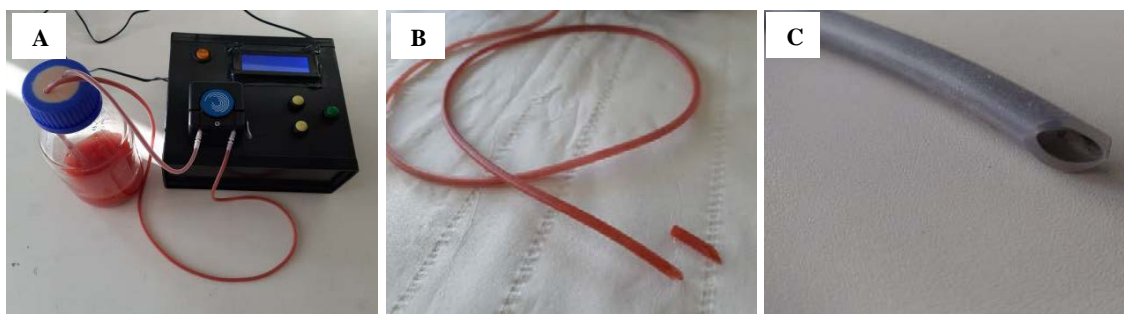

Figure 5: **Preparation of silicone and PVC tubes coated with SeNPs**

SEM analysis with EDS have also indicated the coating density of PVC and silicone surfaces covered with selenium nanoparticles. The scanning electron microscopic analysis is the most crucial technique for the characterization of nanomaterials. PVC tubes are coated with selenium nanoparticles with a size of 100–200 nm, and these single and small particles attach to form more significant clusters with a size of 2 µm (Figure 6). These structures are detected in the top-down and cross-sectional areas and are unevenly and sparsely distributed within the tube. The silicone surface was also coated with a large number of selenium nanoparticles and are evenly distributed over all surfaces (Figure 7A). The thickness of the nanolayer is approximately 16 µm (Figure 7B).
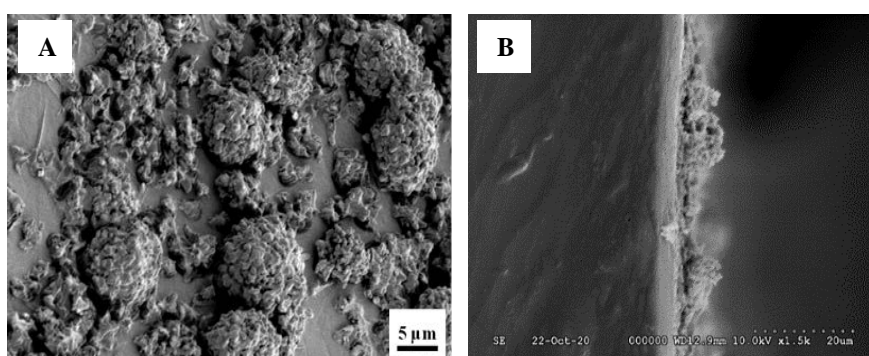

Figure 6: **SEM images for top-down (A), and cross-sectional areas (B) of PVC surface coated with SeNPs**
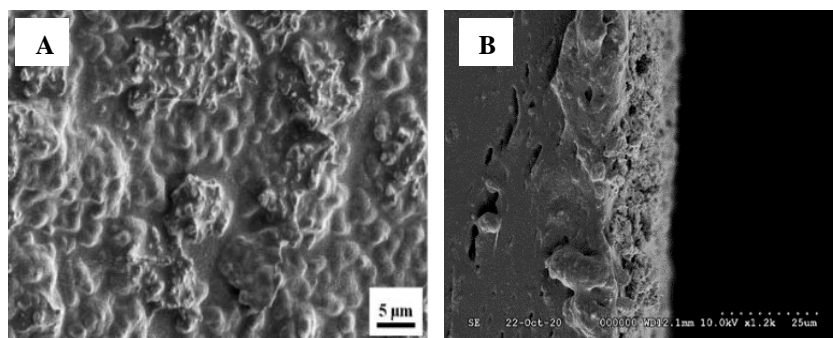
Figure 7: **SEM images for top-down (A), and cross-sectional areas (B) of silicone surface coated with SeNPs**

3.3. Production of selenium nanopowder

Red and grey selenium nanopowder

Red selenium nanoparticles in an aqueous form were produced by reacting 500 mg/L of sodium selenite and 10 g/L of ascorbic acid, which was detailed in section 3.1. Grey hexagonal selenium in aqueous form was converted at the high temperature of 85 °C for 10 minutes from red selenium solution (Figure 8). The grey hexagonal form is the thermodynamically stable form of selenium on the room temperature.
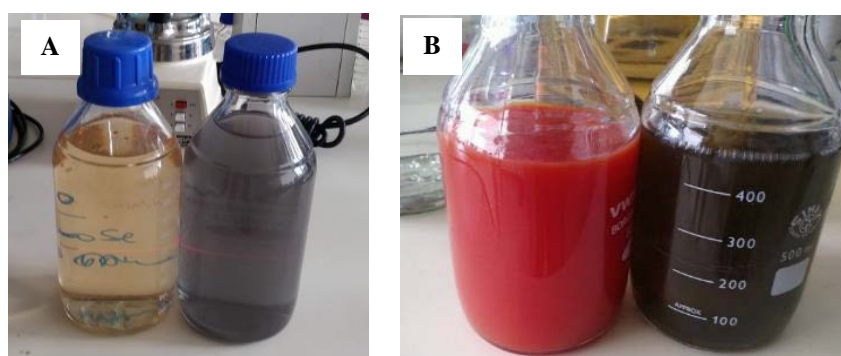

Figure 8: **Red and grey selenium nanoparticles 20 (A) and 200 mg/L of Se (B)**

Selenium nanoparticles in powder form were produced by precipitation, which is the chemical modified method. In a typical procedure, an equal amount of 10,000 mg/L sodium selenite and 100 g/L ascorbic acids were mixed and maintained at ambient temperature for 2 hours. After 30 minutes of the reaction time, the precipitation of the nanogranules began (Figure 9B), and after 2 hours, they were utterly precipitated, as presented in Figure 9C. Then, the nanogranules were removed by filtration and purified by washing with ethanol and distilled water three times (Figure 9D, E). The purified

nanogranules were split to make red selenium nanopowder (red-SeNPs) and grey selenium nanopowder (grey-SeNPs). Red selenium nanogranules were placed at 4 °C until dry (Figure 9F). Grey selenium nanogranules were transformed from red by heating at 85 °C for 10 minutes and dried at room temperature (Figure 9G). Finally, selenium nanogranules were ground using a nano grinder. It is possible to obtain approximately 5 grams of red or grey pure selenium nanopowder from 1000 ml of the aqueous form containing selenium nanoparticles with sizes ranging from 100 nm to 100 µm.
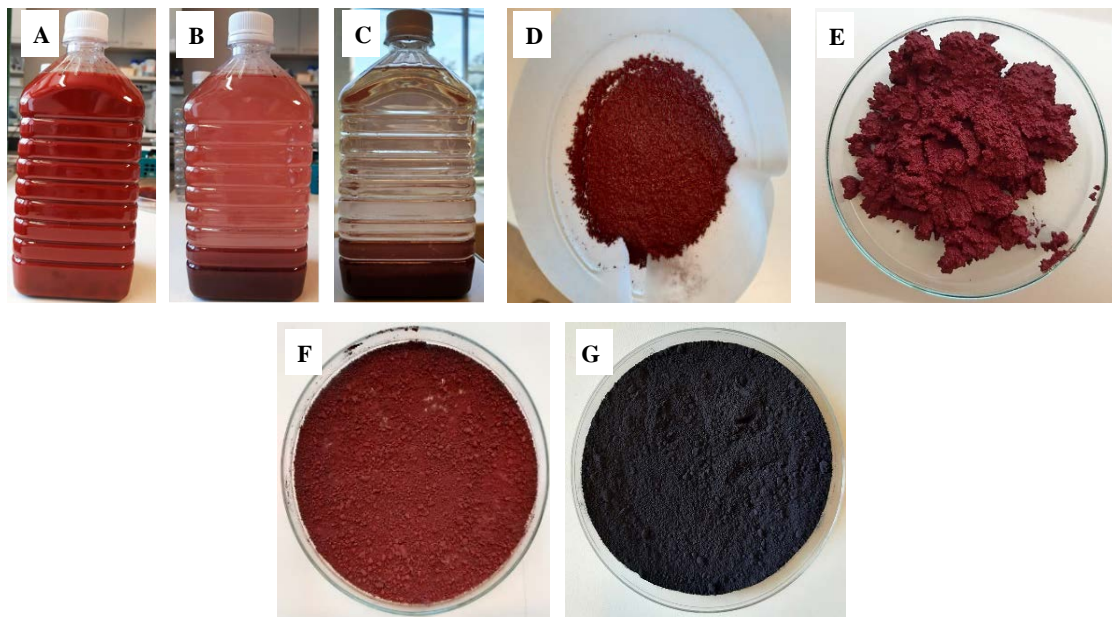

Figure 9: **Schematic illustration (A-G) of the preparation process for red-SeNPs and grey-SeNPs in powder form**

Selenium-enriched yogurt powder

Probiotic yogurt was prepared by bacterial fermentation at incubation at 37 ℃ for 24-36 hours with 1000 mL of skim milk, 200 mg/L of sodium selenite, and starter culture (Lyofast Y 250: *Streptococcus thermophilus* and *Lactobacillus delbrueckiis sp. Bulgaricus*). After incubation, the yogurt turned red, and ascorbic acids (10 mg/L) in powder was added to them. If there is precursor selenium in yogurt, it will be converted into them, also supported extracellular synthesis. Subsequently, the yogurt was maintained at room temperature for 30 minutes and placed in a lyophilizer to obtain a powder (Figure 10).
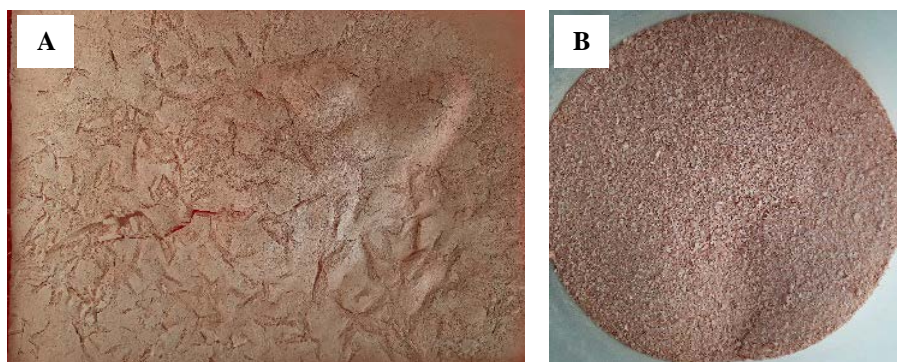
Figure 10: **Selenium-enriched yogurt powder after lyophilization (A), and grinding (B)**

In this case, we can obtain around 120 grams of yogurt powder rich in selenium from 1000 mL of skim milk. This yogurt powder contains about 2000 mg/kg of selenium within 93.8% nano form. During the incubation time, the transformation of selenium nanoparticles with a size ranging 50–500 nm occurred mainly intracellularly in bacteria, confirmed by transmission electron microscopic (TEM) and DLS techniques (Figure 11).
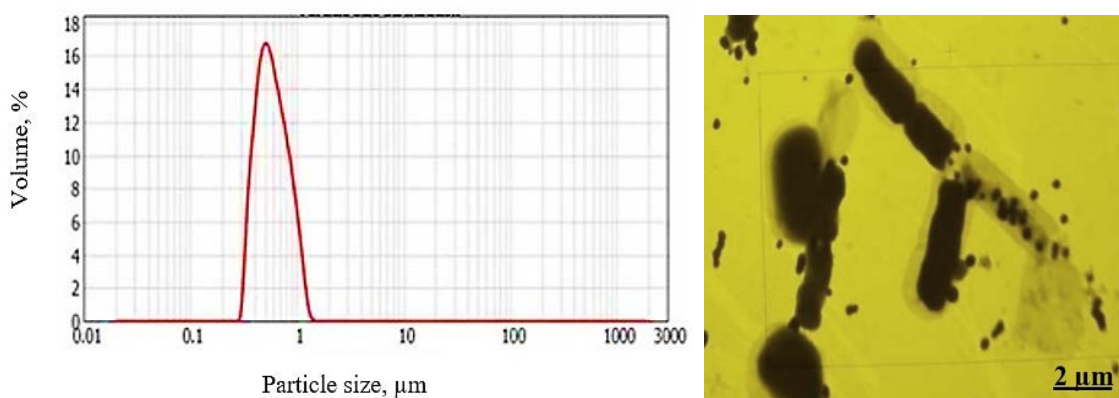

Figure 11: **The particle size distribution of the biosynthesized SeNPs and TEM image of bacteria with SeNPs**

X-ray diffraction analysis with selected area electron diffraction (SAED) and SEM analysis has been used to examine the composition and phase of resultant samples of selenium nanoparticles. The typical XRD pattern of the red selenium synthesized by the chemical method was noisy and broader, with no sharp Bragg reflections indicating the amorphous nature of the particles, as presented in Figure 12A. In the biological synthesis, the amorphous shape of individual nanoparticles and clustered selenium nanoparticles was also confirmed by SEM imaging after purification from the bacterial mass (Figure 12B).
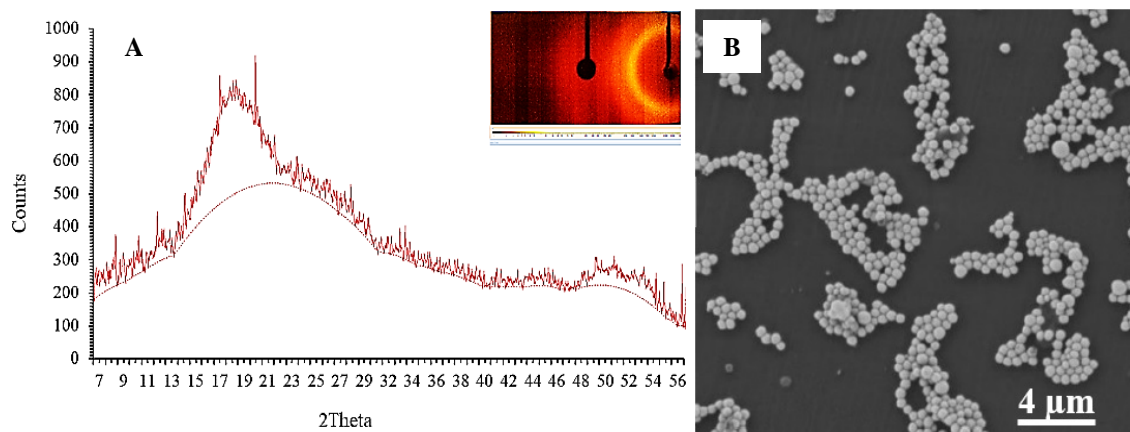
Figure 12: **XRD pattern with the corresponding SAED, and SEM image of red-SeNPs synthesized by chemical (A), biological (B) method**

The grey hexagonal structure of the synthesized selenium nanoparticles (grey-SeNPs) was also confirmed by XRD technique and SEM analysis. The sharps and narrow peaks were detected, and impurities peaks were not observed, which indicates the formation of high purity and well- crystallized selenium nanoparticles after heating at 85 °C for 10 minutes. Figure 13A shows the peaks of selenium are 23.5º, 29.7º, 41.4º, 43.6º, 45.4º, 51.8º, 55.9º, 61.5º, 65.3º, and 71.5º centered at 2θ, that has corresponded to the reflections (100), (101), (110), (102), (111), (201), (112), (202), (210) and (113), which is indication pure hexagonal phase of selenium crystalline form. The lattice parameters were a = 4.366 A° and c = 4.9536 A° (JCPDS 06-0362) (DWIVEDI et al., 2011; CHEN et al., 2011; SRIVASTAVA and MUKHOPADHYAY, 2015).
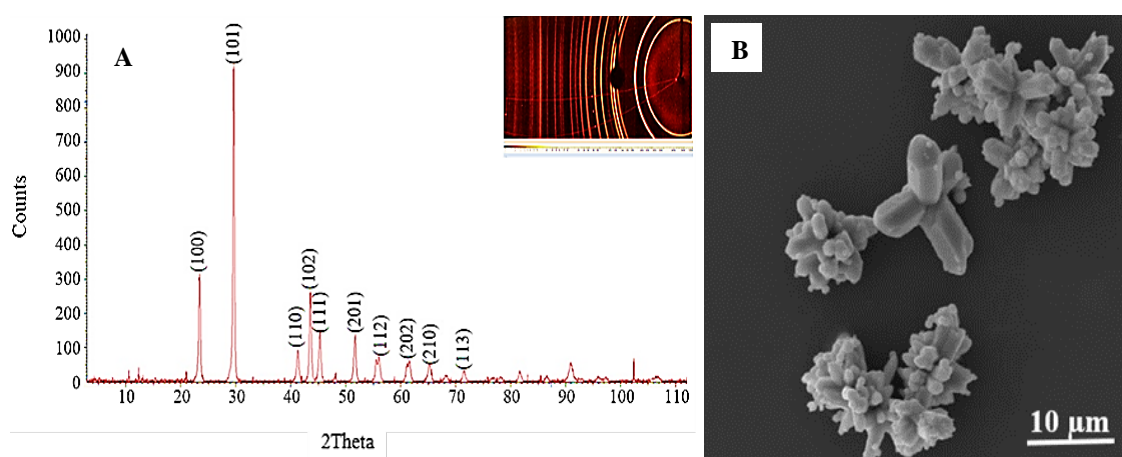

Figure 13: **XRD pattern with the corresponding SAED, and SEM image of grey-SeNPs synthesized by chemical (A), biological (B) method**

3.4. Determining the protective effect of selenium nanoparticles

The homogenous solution of red amorphous selenium nanoparticles with a size 250 nm size was produced by the method, which was patented by Prokisch and Zommara (US8003071B2). The characterization of selenium nanoparticles was already published by ESZENYI et al. (2011), and PROKISCH and ZOMMARA, (2011). They have already shown higher antioxidant activity than other selenium compounds in animal experiments with sheep, chicken, and fish (BENKŐ et al., 2012; UNGVÁRI et al., 2013; GULYÁS et al., 2016). In this experiment, the toxic and antidote effects of such biosynthesized selenium nanoparticles were determined in the animal model organism. *P. caudatum* was fed by adding the same amount of nano-selenium solution to the culture before 2 hours of the experiment.

Toxic concentrations of selenium nanoparticles and toxic substances

It was found that selenium nanoparticles above 800 mg/L had no toxic effects on the morphology and locomotion of *P. caudatum*. They like to eat selenium nanoparticles, and after 5 minutes the selenium particles accumulate inside the cells. The selenium nanoparticles inside Paramecium are shown as dark and yellow spots by the processed light microscope and SEM microscope, as displayed in Figure 14.
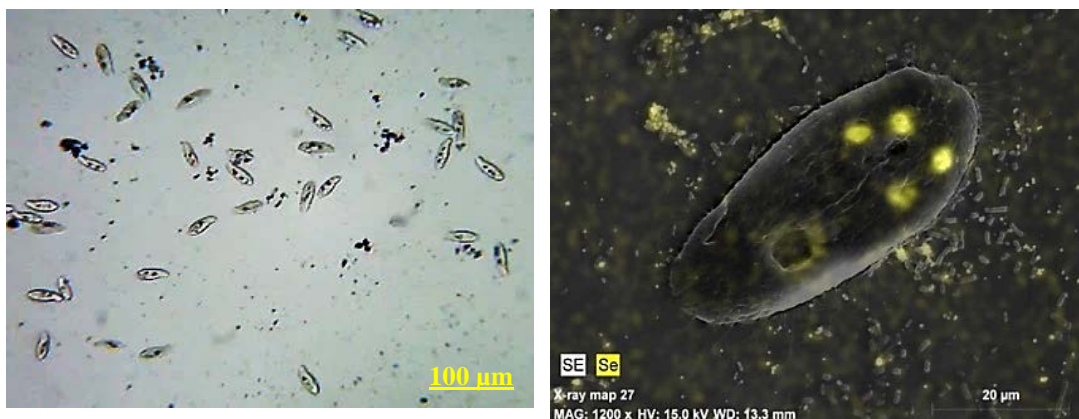

Figure 14: **Optical (A) and SEM images with X-ray (B) of *P. caudatum* treated with SeNPs**

X-ray fluorescence mapping indicates the location of selenium on the image and shows ciliates, selenium spheres, and lactobacillus cells. In other words, These images show no morphological changes in the *P. caudatum* after supplementation with selenium

nanoparticles. Therefore, this result indicates that biosynthesized selenium nanoparticles have no toxic effects on unicellular organisms.

In our study, the lethal effect of toxic substances on *P. caudatum* was determined, as presented in Figure 15: for bulk selenium; ≥10.0 mg/L as sodium selenite, ≥20.0 mg/L as sodium selenate, and for silver; ≥1.25 mg/L of silver nanoparticles, and ≥2.50 mg/L as silver nitrate. All cells have died caused by lysis under 18 minutes. The concentration vs survival time has a unique shape that resembles a pH titration curve, and its turning point gives the LC50 value. Exposure to silver and bulk selenium during the experiment resulted in various changes in locomotion and morphology of Paramecium. Due to the high selenium concentration, Paramecium's swimming stopped completely, but his ciliates continued to move until the cells were lysed. As the concentration decreased, continuous changes in swimming speed, changes (circular motion), immobility, and cytolysis were observed. Swimming speed gradually decreases with increasing exposure time, probably due to the effects of toxicants on cell metabolism and morphological changes. Similar changes in swimming speed, morphological changes, generation time, *etc.* were observed when *P. caudatum* was exposed to high concentrations of insecticide as acephate (VENKATESWARA et al., 2006; 2007). Silver-affected Paramecium showed systematic changes in its shape, primarily by causing irregular bleb formation of the cell membrane before cytolysis. Single or multiple blebs have developed on the cell membrane, which is a common phenomenon during apoptosis. Macronucleus fragmentation and decay were also observed with increasing exposure time. Similar changes in the cell membrane of *P. caudatum* were observed with xenobiotics or insecticides, and they died entirely in 17 minutes (LEON and BERGMANN 1968; VENKATESWARA et al., 2007; RAO et al., 2008).

The antidote effects of selenium nanoparticles

In the experimental group supplemented with selenium nanoparticles, the lethal concentrations of toxic substances were significantly reduced 2-fold. In detail, the lethal concentrations of toxic substances after supplementation found silver nanoparticles at ≥2.5 mg/L, silver nitrate at ≥5.0 mg/L, sodium selenite at ≥20.0 mg/L, and sodium selenate at ≥40.0 mg/L. All cells have survived for an experimental time under the influence of pre-determined lethal concentrations of toxicants. They also did not show any alterations in locomotion and morphology, including shape, blebbing, lysis, and

swimming. In addition, the aforementioned morphological changes lasted longer in the experimental group under the influence of higher than lethal concentrations compared to the control group. Surprisingly, the survival time of Paramecium was extended by the supplementation of nano selenium when exposed to all concentrations of toxicants. Figure 15 shows the experimental and control groups' concentration and survival time changes. Other studies reported that selenium nanoparticles dramatically reduced bulk selenium-induced acute toxicity by up to 4-fold in rodent models (ZHANG et al., 2001), and bulk selenium as selenite was more toxic than nano form in order of adverse effects on mouse growth, liver function, and hepatic lipid peroxidation (ZHANG et al., 2005).
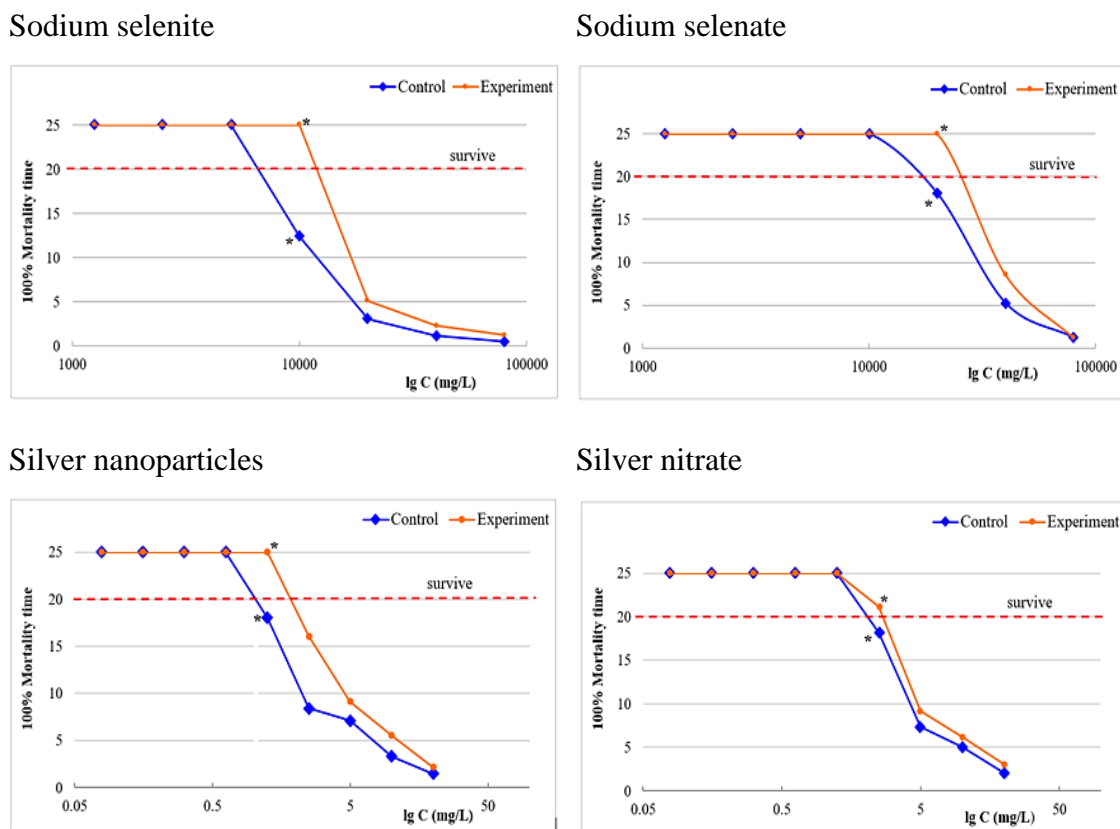
Sodium selenite

Sodium selenate

Silver nanoparticles

Silver nitrate

Figure 15: **The correlation between concentration and survival time on a logarithmic scale. *P. caudatum* was supplemented with SeNPs in experimental groups, and control groups not receiving SeNPs**

The detoxifying effect of selenium nanoparticles can be explained by restoring target selenoprotein activity and restoring the intracellular redox balance. Impairment of the thioredoxin (Trx) and glutaredoxin (Grx) systems allow intracellular ROS and RNS (reactive nitrogen species) proliferation, leading to mitochondrial damage, lipid

peroxidation, calcium homeostasis disorders, protein repair disorders, and cell apoptosis (LU and HOLMGREN 2014). Dietary selenium nanoparticles can be increased antioxidant enzymes including GSH-Px, SOD, and CAT in blood, liver, and kidney (WANG et al., 2007; SHI et al., 2011). The activity of these enzymes plays a critical role in the poisoning.

3.5. Investigation of selenium nanoparticles in nanofiber production

In results, 10% of PVB polymer with a density of 0.81 g mL^{-1} and a viscosity of 474 mm^2 s^{-1} was compatible with a flow rate of 10 mL h^{-1}, a distance of 25 cm between stainless-steel collector and needle tip, and 40 kV of voltage for electrospinning. In addition, the environmental parameters were a humidity of 34% and a temperature of 24 °C. Figure 16 shows the various structures of nanofibers with cylindrical shapes, including linear, spiral, zigzag lines, *etc.* These structures of fiber are visible under a light microscope, and they were taken with white light and red laser lighting.
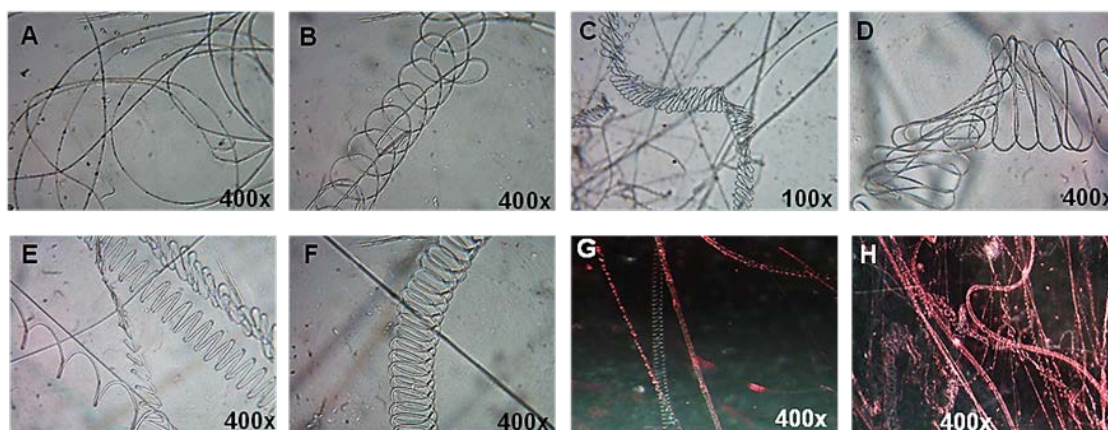

Figure 16: **Optical images of structures of nanofibers enriched with selenium nanoparticles; red-SeNPs (A; B), grey- SeNPs (C; D), aqueous-ethanolic SeNPs (E–H)**

Nanofibers enriched with pre-synthesized selenium nanoparticles

PVB polymer solutions containing 1% to 10% of red-SeNPs and grey-SeNPs were suitable for the formation of nanofibers. Concentrations above 5% of the nanopowder were affected by the viscosity, density, and conductivity of the PVB polymer solution, slowing productivity. As the concentration of selenium nanopowder increases, deeper colored nanofibrous sheets are formed. From light to brighter pink (Figure 17A; B) and

black (Figure 18A; B) nanofibrous sheets with smooth and flexible surfaces originated from 1% and 10% of red-SeNPs and grey-SeNPs. Interestingly, there was no difference in the diameter size, structure, or morphology of the nanofibers produced from the amorphous and crystalline forms of selenium, as well as in the electrospinning process, which was identified by scanning electron microscope with X-ray and EDS (Figure 17C; D and Figure 18C; D). The resulting nanofibers are typically amorphous with a diameter range of 100 nm to 100 µm and a specific surface area of around 4 to 40 $m^2 \ g^{-1}$. Significantly, the mean diameter size was approximately 500 nm with a specific surface area of 8 $m^2 \ g^{-1}$ at all concentrations of selenium nanopowder. In addition, the length of the nanofibers is calculated by the equation for the volume and surface of cylinders, based on their diameter size. As a calculation, the length of the nanofibers is 5093 km cm^{-3} with a diameter of 500 nm, which is derived from 1 mL of 10% polymer solution. The highest concentration of red-SeNPs and grey-SeNPs produced more beads formation than the lowest concentration, which was also confirmed by X-Ray and EDS analysis.
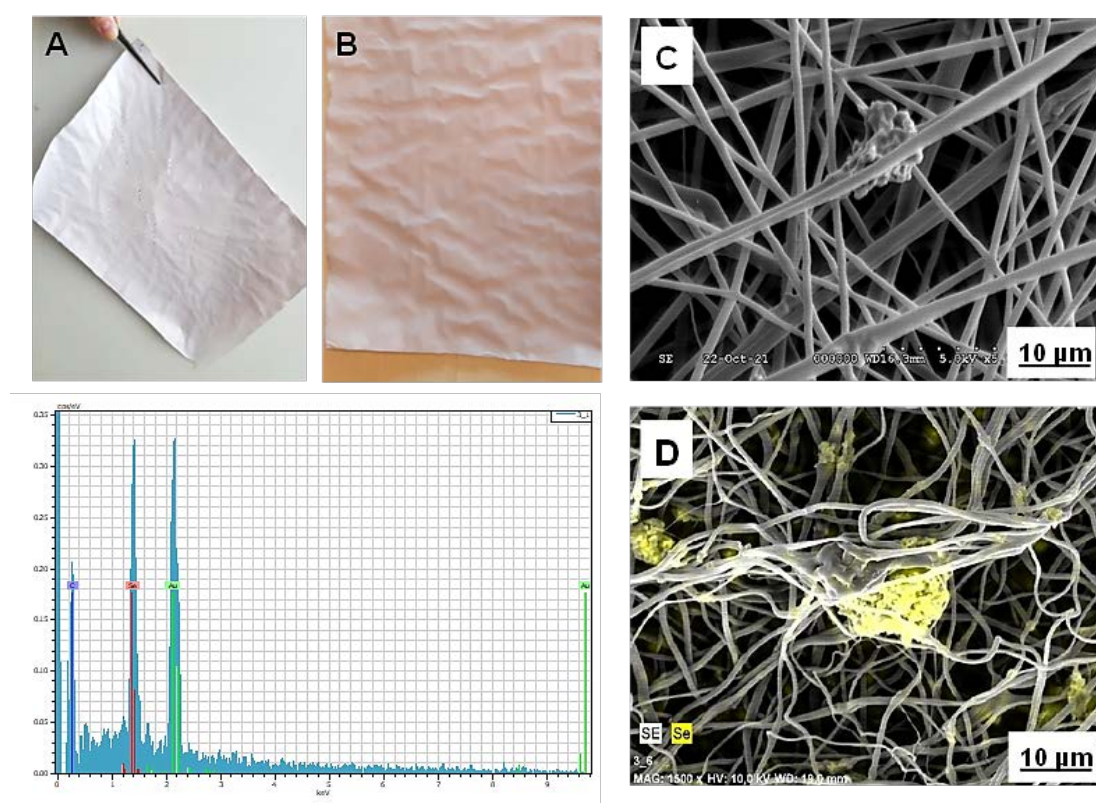

Figure 17: **Nanofibrous sheets enriched with red selenium nanopowder and their SEM images with EDS; (A, C): 1% red-SeNPs, (B, D): 10% red-SeNPs**
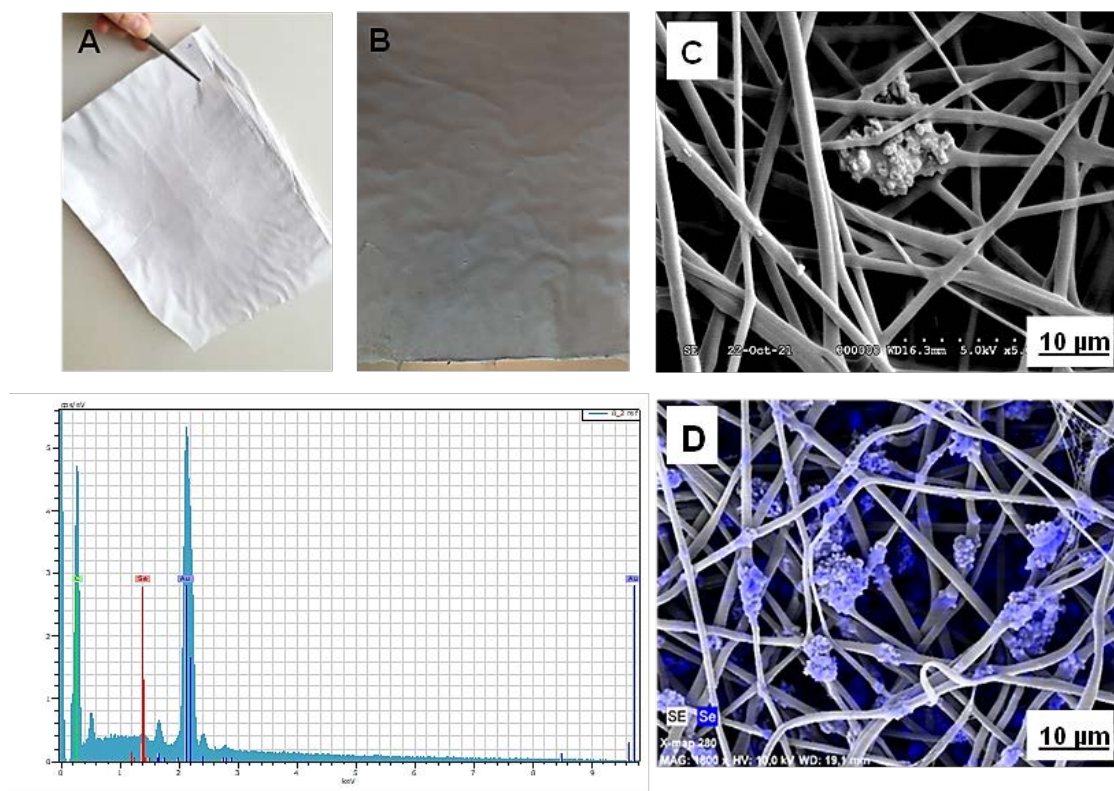
Figure 18: **Nanofibrous sheets enriched with grey selenium nanopowder and their SEM images with EDS; (A, C): 1% grey-SeNPs, (B, D): 10% grey-SeNPs**

Nanofibers enriched with in-situ synthesized selenium nanoparticles

In this section, selenium nanoparticles were synthesized in PVB polymer from a reduction of 500 mg/L sodium selenite by 10 g/L ascorbic acid. A selenium precursor and a reducing agent were dissolved in 80% ethanol at ultrasonic for 30 minutes in a typical procedure. After dissolving, 10% (w/v) of PVB was mixed and treated with ultrasound for 30 minutes. The sodium selenite and the ascorbic acid-enriched PVB polymer solution were stored separately for one day at room temperature. On the next day, these solutions were mixed with ultrasound in equal proportions for 30 minutes to synthesize selenium nanoparticles (SeNPs-PVB). After ultrasonication, the mixture turned red, indicating the formation of selenium nanoparticles, as discussed above. Before electrospinning, this solution was diluted in equal proportions with pure PVB polymer solution to reduce the water phase. Eventually, a pink nanofibrous sheet with a smooth and soft surface containing 1250 mg/L of selenium was produced by electrospinning under the same conditions, as exhibited in Figure 19A. The morphology and diameter size of fiber, and position of the nanoparticles was characterized by SEM. The electrospun nanofibers are

also amorphous with 500 nm of average diameter size. Their length and specific surface area are also similar to nanofibers enriched with selenium nanopowder. Interestingly, nanofibers have contained 50 nm or more small sizes of selenium nanoparticles only inside. The SEM images with low and high magnification showed no particles on the outside of the fiber, as presented in Figure 19B-D.
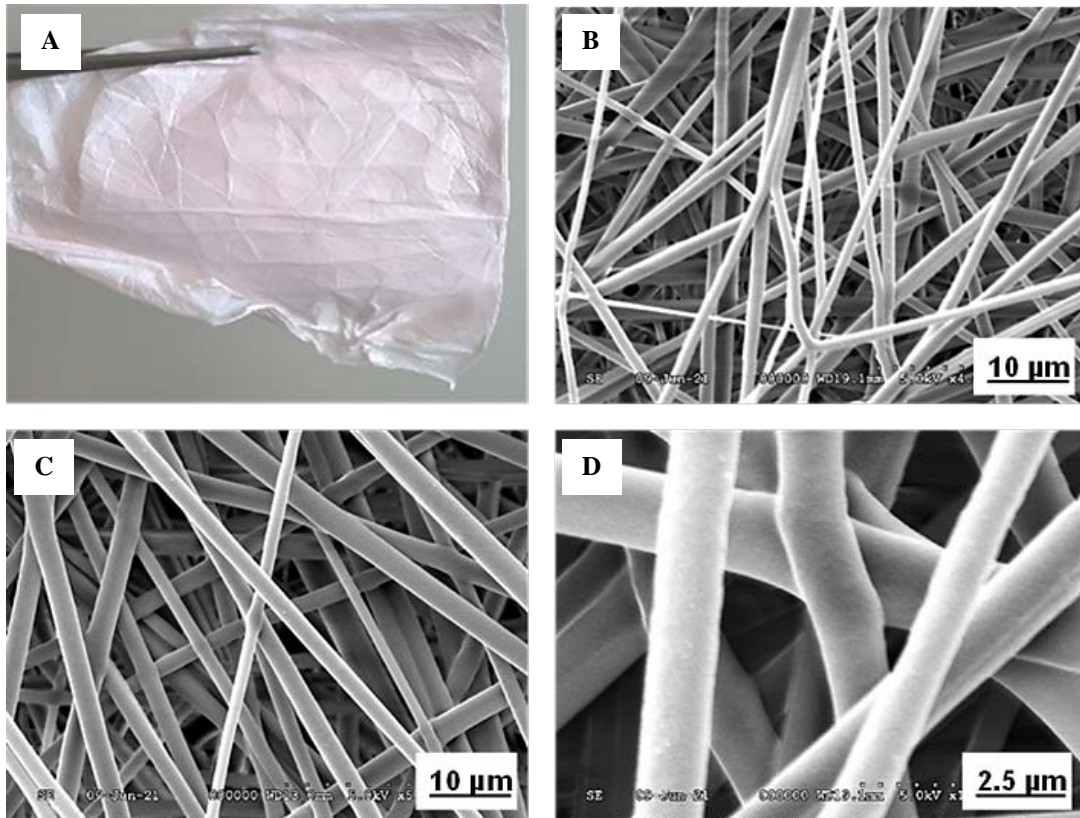

Figure 19: **Nanofibrous sheet enriched by in-situ synthesized SeNPs and its SEM images**

4. NEW SCIENTIFIC RESULTS

1. Red amorphous selenium nanoparticles with sizes ranging from 100 nm to 100 µm in aqueous and powdered form were produced by reacting sodium selenite and ascorbic acid at low (500 mg/L Se with 10 g/L ascorbic acids) and high (10,000 g/L Se with 100 g/L ascorbic acids) concentrations, respectively. Grey hexagonal selenium nanoparticles in aqueous and powdered form were converted by heat treatment at 85 °C for 10 minutes.

2. A homogeneous nanolayer of selenium nanoparticles with a thickness of 16 µm on the inner surface of the silicone tube and an aggregate of 2 µm on the inner surface of the PVC tube was created in a simple and rapid method.

3. The biosynthesized selenium nanoparticles at 800 mg/L have shown no toxic effect on *Paramecium caudatum*. Moreover, they have shown an antidote effect on the silver- and selenium-mediated toxicity of *Paramecium caudatum*. The supplementation with selenium nanoparticles reduced the lethal concentrations of sodium selenite, sodium selenate, silver nanoparticles, and silver nitrate by 2-fold compared to the un-supplemented group. In addition, the survival time of Paramecia was significantly extended by supplementation with selenium nanoparticles.

4. Different types of selenium nanoparticles enriched nanofibers in amorphous shape with a main diameter of 500 nm and a specific surface area of 8 m^2 g^{-1} were produced by the electrospinning technique. 10% of PVB polymer is an excellent matrix for forming nano selenium-enriched nanofibers and nanofibrous sheets.

5. PRACTICAL APPLICABILITY OF RESULTS

1. Comparative studies of aqueous and powdered nano selenium in animal supplements will be needed in the future.

2. Nano selenium coated tubes could fortify the water system in the animal houses and greenhouse. In this case, selenium nanoparticles can show functional effects such as disinfection and enrichment in water. Plants and animals can uptake the selenium nanoparticles without any toxicity from the water. Furthermore, it could be fascinating to use in medicine and microbiological research such as cell culture, ventilators, etc.

3. A method with *Paramecium caudatum* could be suitable for chemical education and toxicological research, such as testing the acute toxicity of toxic metals, metalloid compounds, mycotoxins, insecticides, etc.

4. Nano selenium-enriched nanofibers can be used as medical pads, sponges, rolls for animal treatment, filter membranes for air and water treatment, and as protective fibers against environmental hazards such as chemical and biological or biochemical hazards.

6. REFERENCES

1. BENKO, I. – NAGY, G. – TANCZOS, B. – UNGVARI, E. – SZTRIK, A. – ESZENYI, P. – PROKISCH, J. – BANFALVI, G. (2012): Subacute toxicity of nano-selenium compared to other selenium species in mice. Environmental Toxicology and Chemistry. 31(12), 2812–2820.

2. CHEN, H. – YOO, J. B. – LIU, Y. – ZHAO, G. (2011): Green synthesis and characterization of se nanoparticles and nanorods. Electronic Materials Letters. 7(4), 333-336.

3. DWIVEDI, C. – SHAH, C.P. – SINGH, K. – KUMAR, M. – BAJAJ, P.N. (2011): An organic acid-induced synthesis and characterization of selenium nanoparticles. Journal of Nanotechnology. Article ID 651971, 1–6.

4. ESZENYI, P. – SZTRIK, A. – BABKA, B. – PROKISCH, J. (2011): Elemental, nano-sized (100–500 nm) selenium production by probiotic Lactic acid bacteria. International Journal of Bioscience, Biochemistry and Bioinformatics. 148-152.

5. GULYÁS, G. – CSOSZ, E. – JOE, P. – JÁVOR, A. – MEZES, M. – ERDELYI, M. – BALOGH, K. – JANAKY, T. – SZABO, Z. – SIMON, Á. – CZEGLÉDI, L. (2016): Effect of nano-sized, elemental selenium supplement on the proteome of chicken liver. Journal of Animal Physiology and Animal Nutrition. 101, 502–510.

6. HAGEMAN, S.P.W. – VAN DER WEIJDEN, R.D. – STAMS, A.J.M. – BUISMAN, C.J.N. (2017): Bio-production of selenium nanoparticles with diverse physical properties for recovery from water. International Journal of Mineral Processing. 169, 7–15.

7. LEON, S.A. – BERGMANN, F. (1968): Properties and biological activity of a new peptide antibiotic (Colisan). Biotechnology and Bioengineering. 10(4), 429–444.

8. LIN, Z.H. – CHRIS WANG, C.R. (2005): Evidence on the size-dependent absorption spectral evolution of selenium nanoparticles. Materials Chemistry and Physics. 92(2–3), 591–594.

9. LU JUN. – ARNE HOLMGREN. (2014): The thioredoxin antioxidant system. Free Radical Biology and Medicine, Antioxidants. 66 (January), 75–87.

10. MARTIN, R.B. – PHILIP, J. W. – ROSIE, J.B. – MARK, C.M. – HELEN, C.B. – SARAH, E.J. – MALCOLM, J.H. – STEVE, P.M. – FANG-JIE, Z. – NEIL, B. –

MILES, H. – MARK, T. (2006): Biofortification of UK food crops with selenium. Proceedings of the Nutrition Society. 65(2), 169–181.

11. PROKISCH, J. – ZOMMARA, M. (2011): Process for producing elemental selenium nanospheres. 2011.08.23. Patent No. US 8003071 B2.

12. P.S. ANALYTICAL. (1999): APP092: Using the Millenium Excalibur for selenium speciation. P.S. Analytical Application Notes, Kent, UK

13. RAO, J. VENKATESWARA. – AREPALLI, S.K. – GUNDA, V.G. – BHARAT KUMAR, J. (2008): Assessment of cytoskeletal damage in *Paramecium caudatum*: An early warning system for apoptotic studies. Pesticide Biochemistry and Physiology. 91(2), 75–80.

14. RAYMAN, M.P. (2012): Selenium and human health. The Lancet, 379(9822), 1256–1268.

15. ROEKENS, E.J. – ROBBERECHT, H.J. – DEELSTRA, H.A. (1986): Dietary selenium intake in Belgium for different population groups at risk for deficiency. Diätetische Selen-Aufnahme in Belgien bei verschiedenen Bevölkerungsgruppen mit den Risiken eines Defizits, 182(1), 8–13.

16. SHI, L. – XUN, W. – YUE, W. – ZHANG, C. – REN, Y. – SHI, L. – WANG, Q. – YANG, R. – LEI, F. (2011): Effect of sodium selenite, Se-yeast and nano-elemental selenium on growth performance, Se concentration and antioxidant status in growing male goats. Small Ruminant Research. 96(1), 49–52.

17. SRIVASTAVA, N. – MUKHOPADHYAY, M. (2015): Biosynthesis and structural characterization of selenium nanoparticles using *Gliocladium roseum*. Journal of Cluster Science. 26(5), 1473–1482.

18. UNGVÁRI, EVA. – ISTVÁN MONORI, – ATTILA MEGYERI, – ZOLTAN CSIKI, – JOZSEF PROKISCH, ATTILA SZTRIK, – ANDRÁS JÁVOR, – ILONA BENKŐ. (2013): Protective effects of meat from lambs on selenium nanoparticle supplemented diet in a mouse model of polycyclic aromatic hydrocarbon-induced immunotoxicity. Food and Chemical Toxicology. 64, 298–306.

19. VENKATESWARA RAO, J. – SRIKANTH, K. – AREPALLI, S.K. – GUNDA, V.G. (2006): Toxic effects of acephate on *Paramecium caudatum* with special emphasis on morphology, behaviour, and generation time. Pesticide Biochemistry and Physiology. 86(3), 131–37.

20. VENKATESWARA RAO, J. – GUNDA, V.G. – SRIKANTH, K. – AREPALLI, S.K. (2007): Acute toxicity bioassay using *Paramecium caudatum*, a key member to study the effects of monocrotophos on swimming behaviour, morphology and reproduction. Toxicological & Environmental Chemistry. 89(2), 307–317.

21. WANG, H. – ZHANG, J. – YU, H. (2007): Elemental selenium at nano size possesses lower toxicity without compromising the fundamental effect on selenoenzymes: Comparison with selenomethionine in mice. Free Radical Biology and Medicine. 42(10), 1524–1533.

22. ZHANG JINSONG. – XUEYUN GAO. – LIDE ZHANG. – YONGPING BAO. (2001): Biological effects of a nano red elemental selenium. BioFactors. 15(1), 27–38.

23. ZHANG JINSONG. – HUALI WANG. – XIANGXUE YAN. – LIDE ZHANG. (2005): Comparison of short-term toxicity between nano-se and selenite in mice. Life Sciences. 76(10), 1099–1109.

24. ZHANG, J. – WANG, X. – XU, T. (2008): Elemental selenium at nano size (Nano-Se) as a potential chemo preventive agent with reduced risk of selenium toxicity: Comparison with Se-Methylselenocysteine in mice. Toxicological Sciences. 101(1), 22–31.

PUBLICATION LIST

UNIVERSITY of DEBRECEN

Registry number: DEENK/217/2022.PL
Subject: PhD Publication List

Candidate: Khandsuren Badgar
Doctoral School: Doctoral School of Animal Husbandry
MTMT ID: 10065278

List of publications related to the dissertation

Foreign language scientific articles in Hungarian journals (3)

1. **Badgar, K.**, Prokisch, J.: A simple method for preparing elemental selenium nano- coating inside a silicone surface.
   Acta agrar. Debr. 2021 (1), 35-43, 2021. ISSN: 1587-1282.
   DOI: http://dx.doi.org/10.34101/actaagrar/1/8940

2. **Badgar, K.**, Prokisch, J.: Preparation of red and grey elemental selenium for food fortification.
   Acta Aliment. 50 (2), 289-298, 2021. ISSN: 0139-3006.
   DOI: http://dx.doi.org/10.1556/066.2020.00332
   IF: 0.65 (2020)

3. **Badgar, K.**: The synthesis of selenium nanoparticle (SeNPs) - Review.
   Acta agrar. Debr. 1, 5-8, 2019. ISSN: 1587-1282.
   DOI: https://doi.org/10.34101/actaagrar/1/2359

Foreign language scientific articles in international journals (7)

4. Elsakhawy, T., Omara, A. E. D., Abowaly, M., El-Ramady, H., **Badgar, K.**, Llanaj, X., Törős, G., Hajdú, P., Prokisch, J.: Green Synthesis of Nanoparticles by Mushrooms: A Crucial Dimension for Sustainable Soil Management.
   Sustainability. 14, 1-27, 2022. ISSN: 2071-1050.
   DOI: http://dx.doi.org/10.3390/su14074328
   IF: 3.251 (2020)

5. **Badgar, K.**, Abdalla, N., El-Ramady, H., Prokisch, J.: Sustainable Applications of Nanofibers in Agriculture and Water Treatment: A Review.
   Sustainability. 14 (1), 1-17, 2022. ISSN: 2071-1050.
   DOI: http://dx.doi.org/10.3390/su14010464
   IF: 3.251 (2020)

6. **Badgar, K.**, Prokisch, J.: Elemental Selenium Enriched Nanofiber Production.
   Molecules. 26, 1-9, 2021. ISSN: 1420-3049.
   DOI: http://dx.doi.org/10.3390/molecules26216457
   IF: 4.411 (2020)

7. **Badgar, K.**, Prokisch, J., El-Ramady, H.: Nanofibers for Sustainable Agriculture: A Short Communication.
   Egypt.J. Soil Sci. 61 (3), 373-380, 2021. EISSN: 2357-0369.
   DOI: http://dx.doi.org/10.21608/ejss.2021.105877.1477

8. **Badgar, K.**, Prokisch, J.: Testing Toxicity and Antidote Effect of Selenium Nanoparticles with Paramecium caudatum.
   Open J. Anim. Sci. 11 (04), 532-542, 2021. ISSN: 2161-7597.
   DOI: http://dx.doi.org/10.4236/ojas.2021.114036

9. **Badgar, K.**, Prokisch, J.: The production methods of selenium nanoparticles.
   Acta Univ. Sapientiae, Alim. 14 (1), 14-43, 2021. ISSN: 1844-7449.
   DOI: http://dx.doi.org/10.2478/ausal-2021-0002

10. **Badgar, K.**, Prokisch, J.: The Effects of Selenium Nanoparticles (SeNPs) on Ruminant.
    Proc. Mong. Acad. Sci. 60 (4), 1-8, 2020. ISSN: 2310-4716.
    DOI: http://dx.doi.org/10.5564/pmas.v60i4.1500

List of other publications

Foreign language scientific articles in international journals (4)

11. El-Ramady, H., Abdalla, N., **Badgar, K.**, Llanaj, X., Törős, G., Hajdú, P., Eid, Y., Prokisch, J.: Edible Mushrooms for Sustainable and Healthy Human Food: Nutritional and Medicinal Attributes.
    Sustainability. 14 (9), 1-30, 2022. ISSN: 2071-1050.
    DOI: http://dx.doi.org/https://doi.org/10.3390/su14094941
    IF: 3.251 (2020)

12. El-Ramady, H., Abdalla, N., Fawzy, Z., **Badgar, K.**, Llanaj, X., Törős, G., Hajdú, P., Eid, Y., Prokisch, J.: Green Biotechnology of Oyster Mushroom (Pleurotus ostreatus L.): A Sustainable Strategy for Myco-Remediation and Bio-Fermentation.
    Sustainability. 14 (6), 1-21, 2022. ISSN: 2071-1050.
    DOI: http://dx.doi.org/10.3390/su14063667
    IF: 3.251 (2020)

13. Saffan, M. M., Koriem, M. A., Elhenawy, A. S., El-Mahdy, S., El-Ramady, H., Elbehiry, F., Omara, A. E. D., Bayoumi, Y., **Badgar, K.**, Prokisch, J.: Sustainable Production of Tomato Plants (Solanum lycopersicum L.) under Low-Quality Irrigation Water as Affected by Bio-Nanofertilizers of Selenium and Copper.
    Sustainability. 14 (6), 1-17, 2022. ISSN: 2071-1050.
    DOI: http://dx.doi.org/10.3390/su14063236
    IF: 3.251 (2020)
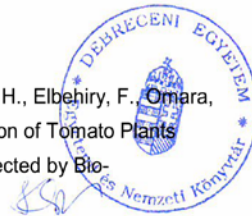
14. Prokisch, J., **Badgar, K.**, El-Ramady, H.: Fortification of Functional Foods for Human Health: A Case Study of Honey and Yogurt for Diabetes.
Env. Biodiv. Soil Security. 5 (1), 331-340, 2021. ISSN: 2536-9415.
DOI: http://dx.doi.org/10.21608/jenvbs.2021.110812.1154

Total IF of journals (all publications): 21,316
Total IF of journals (publications related to the dissertation): 11,563

The Candidate's publication data submitted to the iDEa Tudóstér have been validated by DEENK on the basis of the Journal Citation Report (Impact Factor) database.

25 April, 2022